The Effect of Bubble Surface Area Flux on Flotation Efficiency of Pyrite Particles

Shahbazi, Behzad*+

Department of Mining Engineering, Science and Research Branch, Islamic Azad University, Tehran, I.R. IRAN

Rezai, Bahram

Mining Engineering Department, Amirkabir University of Technology, Tehran, I.R. IRAN

Koleini, Sayed Mohammad Javad

Mining Engineering Department, Tarbiat Modares University, Tehran, I.R. IRAN

Noparast, Mohammad

Mining Engineering Department, University of Tehran, Tehran, I.R. IRAN

ABSTRACT: *In this research, the effect of bubble surface area flux, S_b, and particle size on flotation rate constant, k, of pyrite (FeS_2) particles was studied using bubble-particle interactions. The bubble-particle collision, attachment and detachment efficiencies were calculated under different flow regimes. The k increased with increase in the collision efficiency and decrease in the detachment efficiency. Also the bubble-particle collection efficiency increased with increase in the S_b. Thus difficulty in the floating of fine particles was attributed to low efficiency of the bubble-particle collision efficiency while difficulty in the floating of coarse particles was due to high efficiency of bubble-particle detachment. Maximum collision, attachment and detachment efficiencies were obtained as 81.57%, 50.60% and 51.89%, respectively.*

KEY WORDS: *Flotation, Pyrite, Collision, Attachment, Detachment.*

INTRODUCTION

A key element of the effectiveness of the recovery of valuable minerals via the flotation process is the interaction between particles and air bubbles. The bubble–particle interaction involves a number of micro processes, which can be divided into collision, attachment and detachment. Despite recent advances, these micro processes are still not well understood from a quantitative viewpoint [1].

Froth flotation is widely used for separating different minerals from each other. However, its effectiveness is limited to a relatively narrow particle size range of 10-100 μm [2]. Although the effect of particle size on flotation performance has been widely studied and many important physico-chemical factors related to particle size have been identified [2-10], the net effect of these factors is very difficult to predict. For example, in bubble-particle

* *To whom correspondence should be addressed.*
+ *E-mail: bzshahbazi@yahoo.com*
1021-9986/13/2/109 10/$/3.00

interaction, particle size is known to play a critical role in the efficiency of particles colliding with bubbles, attachment of particles to bubbles after collision, as well as remaining attached in the pulp phase [11, 12].

The surface area flux work has been published in a series of papers [13-18]. For instance, *Gorain et al.* (1997) have investigated the effect of gas dispersion properties on the flotation rate constant, k, in plant and pilot scale mechanical cells over a range of operating conditions for four impeller types [17]. They found that the k is not readily related to the bubble size, gas holdup or superficial gas velocity individually, but it is related to the bubble surface area flux, S_b, that the relationship is linear for shallow froths. It has also been found that S_b was strongly related to the k and that the relationship is linear, as represented by the following equation [17, 18]:

$$k = \alpha R_f S_b \quad (1)$$

$$S_b = 6J_g / d_{32} \quad (2)$$

Where, J_g is the superficial gas velocity, d_{32} is the Sauter mean diameter of the bubbles, α is the floatability factor, which encompasses the contribution of particle size and hydrophobicity [19], and R_f is the froth recovery factor, which is defined as the ratio of the overall flotation rate constant and the collection zone rate constant [18].

In this research, the effect of S_b and particle size on the k of pyrite (FeS_2) particles is studied. So the relationship between k and S_b is studied using bubble-particle interactions and, consequently, has important implications regarding the optimization, scale-up and design of mechanical flotation cells.

EXPERIMENTAL SECTION

Flotation experiments were carried out in a mechanical laboratory flotation cell. An impeller diameter of 0.07 m was used for pulp agitation and a cell with square section was used in which the length and height were 0.13 and 0.12 m, respectively. The impeller rotating speed was 900, 1000, 1100 and 1200 rpm and the air flow rate was 120 and 180 l/h. Pyrite (FeS_2) particles of eight size classes containing -37, -53+37, -75+53, -106+75, -212+106, -300+212, -420+300 and -500+420 μm were used for flotation experiments. Chemical composition of the pyrite sample is given in Table 1. The frother was

Table 1: Chemical composition of Pyrite used in the experiments (XRF).

Chemical Composition	Wt%
Fe	45.95
S	43.78
SiO_2	1.19
CaO	0.38
Cu	4.03
K_2O	0.45
Al_2O_3	1.25
Loss of ignition (L.O.I.)	2.97

MIBC (methyl iso-butyl carbinol) with the concentration of 22.4 ppm. The flotation experiments were carried out by potassium amyl xanthate collector (200 g/t) at the pH of 9.5 using local tap water. When the S_b values were set, all the size fractions were floated together under those exact conditions (Table 2). Eq. 1 is not universally accepted and certainly can only be valid up to a certain S_b (a limit on the S_b before the cell boils). So, in this investigation, S_b was 16.77 to 27.43 1/s. Also, in all the experiments, the froth depth was shallow and the froth recovery factor, R_f, was assumed to be equal to 1.

The air flow rate and the impeller speed were set and the float product was collected at the time intervals of 2, 4, 6 and 8 minutes. The k was calculated assuming the first order rate equation (Eq. 3) for a batch cell and plotting Eq. 4 versus t (Fig. 1). According to Fig. 1a, flotation recovery after 8 minutes was close to R* approximately.

$$R = R^*(1 - \exp(-kt)) \quad (3)$$

$$\ln(1 - R/R^*) \quad (4)$$

Where R* is infinite recovery. According to Fig. 2, bubble size distribution was measured in a device similar to the McGill's bubble viewer [20]. It consisted of a sampling tube attached to a viewing chamber with a window inclined 15° from vertical. The closed assembly was filled with water of a similar nature to that in the flotation cell (to limit changes in the bubble environment during the sampling). Then the tube was immersed in the desired location below the froth. Bubbles rose into the viewing chamber and were imaged by a digital camera

Table 2: The conditions of flotation experiments.

Gas Flow Rate (L/h)	120	120	120	120	180	180	180	180
Impeller Speed (rpm)	900	1000	1100	1200	900	1000	1100	1200
d_b (μm)	830	750	680	620	820	750	680	620
*ε_g (%)	3.62	4.71	5.93	7.30	4.08	5.29	6.65	8.17
J_g (cm/s)	0.2	0.2	0.2	0.2	0.3	0.3	0.3	0.3
S_b (1/s)	16.77	17.94	19.08	20.19	22.69	24.31	25.89	27.43
Re_b	303	226	171	131	301	224	170	130
**ε (W/kg)	2.15	2.95	4.18	5.98	2.15	2.95	4.18	5.98

*ε_g is gas holdup **ε is energy dissipation

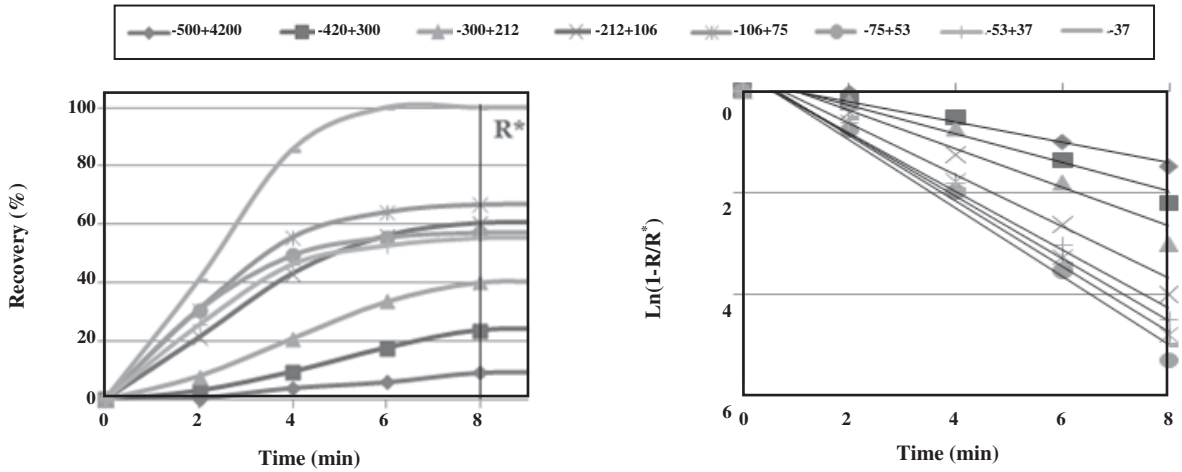

Fig. 1: Calculation of the flotation rate constant base on R* (S_b = 19.08 1/s)

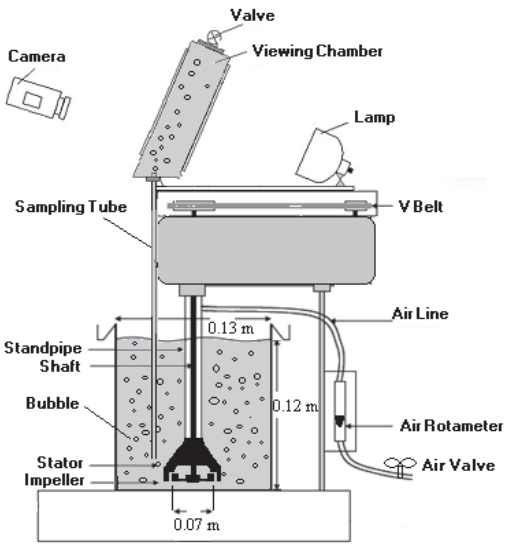

Fig. 2: Bubble diameter measurement for different impeller speeds and air flow rates.

as they slid up the inclined window, which was illuminated from behind [20].

The Washburn method was used to measure contact angle on the powder. Contact angle of pyrite particles was measured using Lauda tensiometer (TE3) after flotation tests. The Lauda tensiometer simplifies the characterization of wetting behavior of the whole surface. The contact angle was measured by means of the precise adjustment of the immersion/receding rate and micrometer-accurate measurement of the immersion dept. Contact angle of the pyrite sample was obtained as 80.7° using Lauda tensiometer (TE3).

Superficial gas velocity was calculated using the air flow rate and the area cross section of the cell with consideration of the area occupied by the impeller shaft. The input power was inferred from the electrical measurements and measuring the entrance amperage and voltage to the electrical motor of the flotation equipment.

THEORITICAL SECTION

The flotation rate constant is proportional to the collection efficiency [21]. This equation can be seen as the equation below [22]:

$$E_{col} = E_c E_a (1 - E_d) \quad (5)$$

Where, E_c is the bubble-particle collision efficiency, E_a is the bubble-particle attachment efficiency and E_d is the bubble-particle detachment efficiency. Equations of the bubble-particle collision, attachment and detachment efficiencies under different flow conditions are given in Table 3. The five parameters of d_b, v_b, v_p, Re_b and t_i are necessary for calculating the collision, attachment and detachment efficiencies that these parameters are obtained using following equations (Eqs. 6-11). The mean bubble diameter adopted was the Sauter diameter, calculated by the equation below [29]:

$$d_b \text{ or } d_{32} = \frac{\sum n_i d_i^3}{\sum n_i d_i^2} \quad (6)$$

Where, n is the number of bubbles and d is the bubble diameter. If the surface of a drop or bubble is immobile for any reason, the floating velocity is the same as that of a solid sphere and the bubble raise velocity can be described by the Stokes' equation [30]:

$$v_b = \frac{d_b^2}{18\nu} g \quad (7)$$

where ν is kinematic viscosity. Also particle settling velocity can be described by the equation below [31]:

$$v_p = \sqrt{\frac{3g(\rho_s - \rho)d_p}{\rho}} \quad (8)$$

Where, neither Newton's nor Stokes' laws apply, rather there is another equation for calculating the particle settling velocity as follows [32]:

$$V_p = \frac{20.52\eta}{d_p \rho}\left(\left[1 + 0.0921\left(\frac{d_p^3(\rho_s - \rho)\rho g}{0.75\eta^2}\right)^{0.5}\right]^{0.5} - 1\right)^2 \quad (9)$$

Where, η is dynamic viscosity. The bubble Reynolds number is another effective hydrodynamic parameter on the k, which is calculated by the equation below [33]:

$$Re_b = v_b d_b \rho / \eta \quad (10)$$

The induction time is a function of the particle size and contact angle, which can be determined by the equation below [34,35]:

$$t_i = \frac{75}{\theta} d_p^{0.6} \quad (11)$$

Where θ is contact angle.

RESULTS AND DISCUSSIONS

Flotation recovery of pyrite particles

With increase in the particle size, the transferring ability of air bubbles reduced to the minimum and therefore flotation recovery decreased. The S_b was increased with increasing the air flow rate. So, the flotation recovery of pyrite particles increased with increasing of the air flow rate and S_b.

The flotation rate of pyrite particles for different particle sizes, air flow rates and impeller speeds is given in Fig. 3. Maximum peaks for the particle size of -37 μm are attributed to the entrainment phenomena. Furthermore, Maximum peaks for particle size of -75+53 μm can be due to both of the increasing attachment efficiency and decreasing detachment efficiency.

The k was increased with increase in the S_b and decrease in the particle size. The maximum k was obtained as 0.67 1/min, when the particle size, impeller speed and S_b were -75+53 μm, 1100 rpm and 19.08 1/s, respectively. The minimum k was obtained as 0.16 1/min

Table 3: Equations for calculating bubble-particle collision, attachment and detachment efficiencies.

Bubble-particle Interaction	Flow Conditions	Equation
Collision Efficiency [23,24]	Flint-Howarth	$E_{c-FH} = \frac{v_p}{v_p + v_b}$
	Stokes	$E_{c-St} = \frac{3}{2}(d_p / d_b)^2$
	Potential	$E_{c-P} = 3d_p / d_b$
	Intermediate	$E_{c-I} = (d_p / d_b)^2 \left[\frac{3}{2} + \frac{4 Re_b^{0.72}}{15} \right]$
Collision Frequency [25]	Saffman-Turner	$Z = \sqrt{\frac{8\pi}{15}} \left(\frac{d_p + d_b}{2} \right)^3 \left(\frac{\varepsilon}{\nu} \right)^{1/2}$
Attachment Efficiency [24,26]	Yoon	$E_{a-Y} = \sin^2 \left[2 \arctan \exp \left(\frac{-(45 + 8 Re_b^{0.72}) v_b t_i}{15 d_b (d_b/d_p + 1)} \right) \right]$
	Stokes	$E_{a-St} = \sec h^2 \left(\frac{2 v_p A_{St} t_i}{d_p + d_b} \right)$, $A_{St} = \frac{v_b}{v_p} + 1 - \frac{3}{4}\left(1 + \frac{d_p}{d_b}\right)^{-1} - \frac{1}{4}\left(1 + \frac{d_p}{d_b}\right)^{-3}$
	Potential	$E_{a-P} = \sec h^2 \left(\frac{2 v_p A_P t_i}{d_p + d_b} \right)$, $A_P = \frac{v_b}{v_p} + 1 + \frac{1}{2}\left(1 + \frac{d_p}{d_b}\right)^{-3}$
Detachment Efficiency [27]	Bloom and Heindel	$E_d = \exp \left[0.5 \left(1 - \frac{1}{Bo^*} \right) \right]$, $Bo^* = \frac{d_p^2 \left[\Delta\rho_s g + 1.9 \rho_s \varepsilon^{\frac{2}{3}} \left(\frac{d_p}{2} + \frac{d_b}{2} \right)^{-\frac{1}{3}} \right]}{6\sigma \sin\left(\pi - \frac{\theta}{2}\right) \sin\left(\pi + \frac{\theta}{2}\right)} + \frac{1.5 d_p \left(\frac{4\sigma}{d_b} - d_b \rho g \right) \sin^2\left(\pi - \frac{\theta}{2}\right)}{6\sigma \sin\left(\pi - \frac{\theta}{2}\right) \sin\left(\pi + \frac{\theta}{2}\right)}$
Detachment Frequency [28]	Mika and Fuerstenau	$Z' = \sqrt{C_1} \varepsilon^{\frac{1}{3}} (d_p + d_b)^{\frac{-2}{3}}$, $1.61 \le C_1 \le 2.33$

v_p: particle velocity, v_b: bubble velocity, d_p: particle diameter, d_b: bubble diameter, t_i: induction time, Re_b: bubble Reynolds number, Bo^*: Bond number, ε: energy dissipation, C_1: empirical value, θ: contact angle, g: acceleration due to gravity, σ: surface tension, ρ_s: particle density, $\Delta\rho_s = (\rho_s - \rho)$, ρ: fluid density, ν= kinematic viscosity

for the particle size of -500+420 μm, impeller speed of 1000 rpm and S_b of 17.95 1/s.

Bubble-particle collision efficiency

In the previous section, the k-S_b relationship for the different impeller speeds and air flow rates was investigated. This section will try to determine the collision efficiency for a better interpretation of the results obtained from the experiments. So far various relations have presented for calculating of the bubble-particle collision efficiency that each of them can be used under certain conditions. In this research, for calculating of the bubble-particle collision efficiency, different relationships are used to determine the appropriate estimates.

Collision frequency for the different energy dissipation and bubble-particle aggregate diameter, d_b+d_p, is shown in Fig. 4. Obtaining the collision frequency involves measuring the energy dissipation in the system.

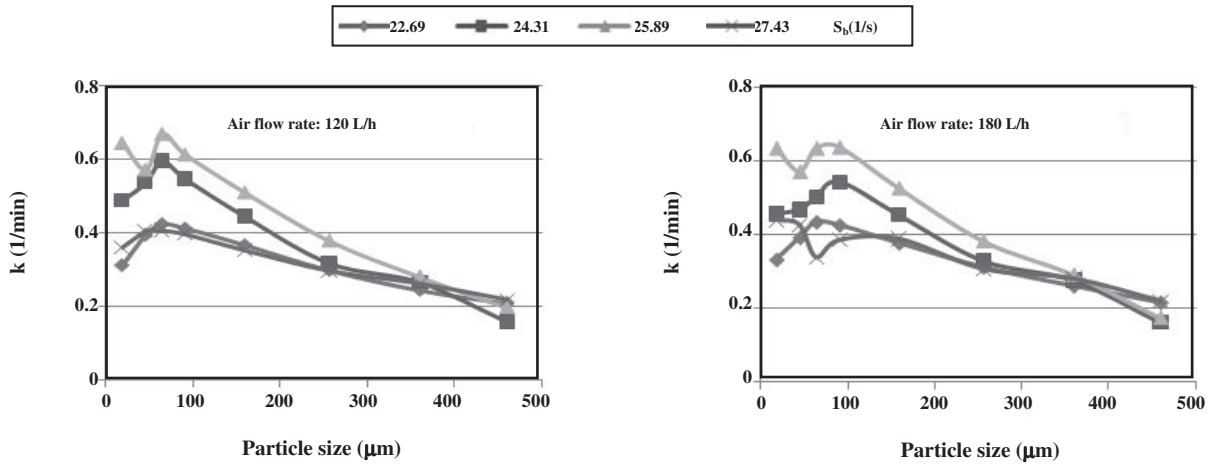

Fig. 3: Flotation rate of the pyrite particles for different amounts of particle sizes, air flow rates and S_b.

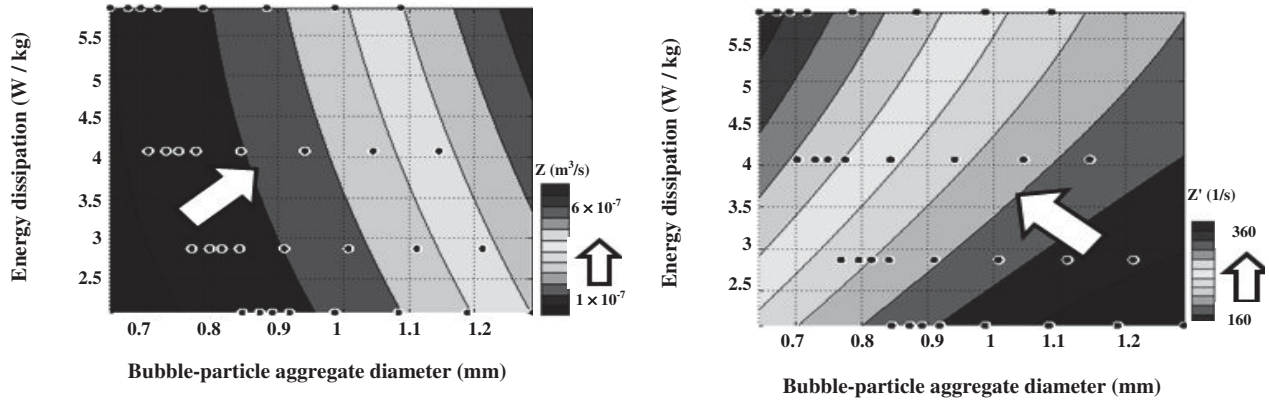

Fig. 4: The effect of energy dissipation and bubble-particle aggregate diameter on the collision and detachment frequencies.

In this study, the energy dissipation was within the range of 2.15-5.98 W/kg and the results showed that the flotation rate of pyrite particles increased with increase in the energy dissipation. The collision frequency was obtained between 10^{-7} to 6×10^{-7} m^3/s. The energy dissipation increased with increase in the impeller speed and thus bubble-particle collision frequency will increase as well. So the collision frequency increased with increase in both the energy dissipation and bubble-particle aggregate diameter.

According to Fig. 5, the Flint-Howarth collision efficiency was calculated for different particle sizes using the first equation of Table 3 ($11.11<E_{c\text{-}FH}<52.56\%$). The bubble-particle collision efficiency increased with increase in both the particle size and S_b. The maximum Flint-Howarth collision efficiency was obtained as 52.56% with the k of 0.22 1/min, S_b of 27.43 1/s and particle size of -500+420 μm. The Flint-Howarth collision efficiency for coarse particles was very lower than that of other models. So perhaps this model is not applicable for coarse particles.

According to Fig. 5, the Stokes' collision efficiency was calculated for different S_b and particle sizes ($0.07<E_{c\text{-}S}<81.57\%$). The maximum Stokes collision efficiency was obtained as 81.57% with the S_b of 27.43 1/s, particle size of -500+420 μmand k of 0.22 1/min. Also the minimum Stokes' collision efficiency was obtained as 0.07% with the particles size of -37 μm and S_b of 16.77 1/min. This model appears to give a good estimation of collision efficiency for both the coarse and fine particles.

Also the collision efficiency was calculated based on the Potential and Intermediate flow conditions (Fig. 5). Both the Potential and Intermediate collision efficiencies

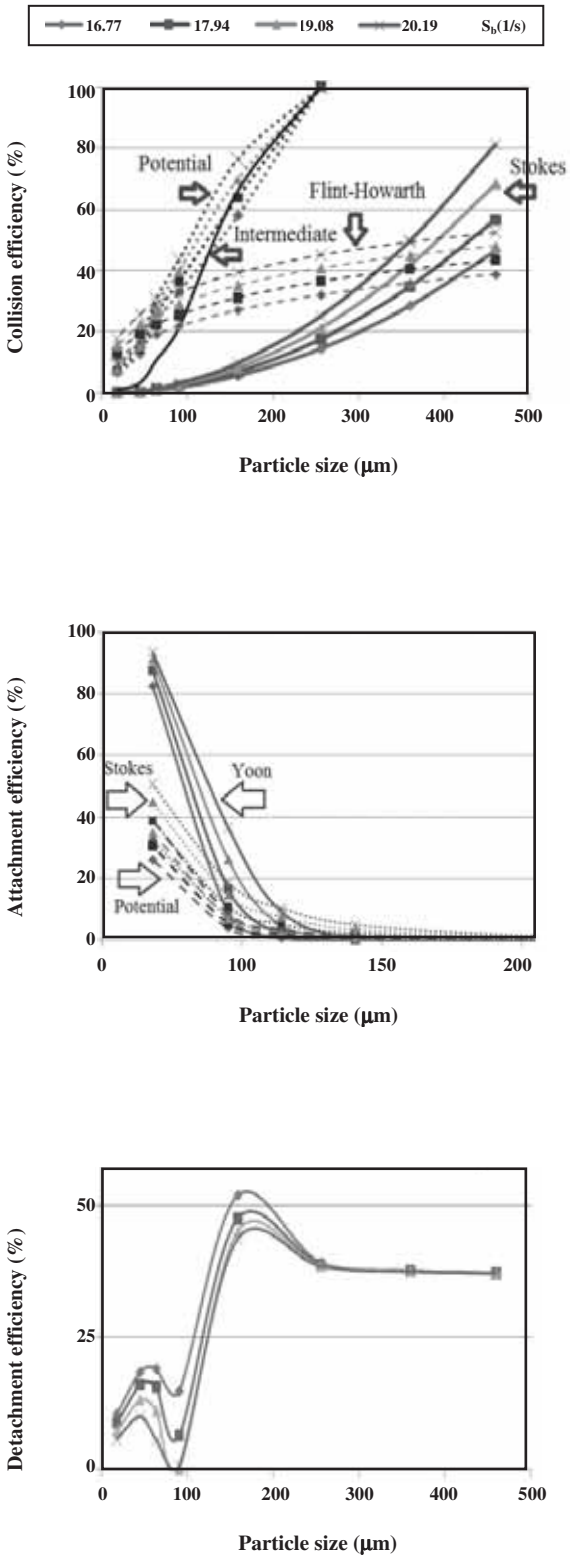

Fig. 5: The effect of S_b and particle size on the bubble-particle collision efficiency.

were exaggerated as the collision efficiency of coarse particles (-300+212, -420+300 and -500+420 μm) was more than 100%. So these models were not applicable for the coarse particles.

Bubble-particle attachment efficiency

The effect of S_b and particle size on the attachment efficiency is shown in Fig. 5. Both the k and attachment efficiency increased with the increasing of the S_b. So increasing of the k can be attributed to increase of the attachment efficiency. Attending to complexity of the attachment equations (Table 3), reason of this fact is not completely clear and it is may be due to decreasing of the bubble diameter and thus decreasing of the bubble rise velocity.

The maximum Yoon's, Stokes' and Potential attachment efficiencies were obtained as 93.52, 50.60 and 39.15%, respectively. The maximum attachment efficiency was obtained with the particle size of -37 μm, S_b of 27.43 1/s and k of 0.44 1/min. Yoon's attachment efficiency was more than the other attachment efficiencies and the attachment efficiencies calculated under the potential flow conditions were very lower than that of both the Yoon's and Stokes' attachment efficiencies.

Bubble-particle detachment efficiency

The effect of energy dissipation on detachment frequency is shown in Fig. 4. In this research, detachment frequency was in the range of 160-360 1/s. The maximum detachment frequency obtained was 360 1/s with the energy dissipation of 5.98 W/kg and bubble-particle aggregate diameter of 0.64 mm. The minimum detachment frequency obtained was 160 1/s with the energy dissipation of 2.15 W/kg and bubble-particle aggregate diameter of 1.3 mm. So, detachment frequency increased with increasing of the energy dissipation and decreasing of bubble-particle aggregate diameter. The k increased with decrease of the detachment frequency.

Detachment efficiency increased with decrease of the S_b. In this research, decrease in the bubble diameter (gas dispersion) is due to increasing of the energy dissipation (ε). According to detachment equation in Table 3, increasing of the detachment efficiency is due to decreasing of the energy dissipation and also should be consider that S_b decreases with decreasing energy dissipation. According to Fig. 5, the maximum

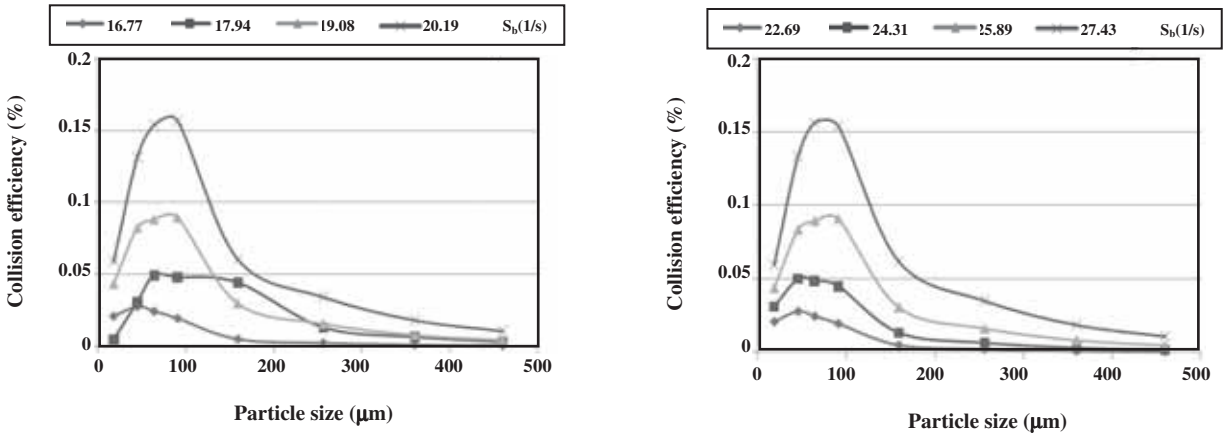

Fig. 6: The effect of S_b and particle size on the bubble-particle collection efficiency.

detachment efficiency was obtained as 51.89% with the S_b of 16.77 1/s, particle size of -212+106 μm and k of 0.37 1/min. Also the minimum detachment efficiency was obtained as 0%, for the particle size of -106+75 μm, S_b of 25.89 1/s and k of 0.64 1/min.

Efficiency of collecting particles with bubbles

The effect of S_b and particle size on bubble-particle collection efficiency is shown in Fig. 6. Since the bubble-particle collision, attachment and detachment efficiencies have already been calculated, now calculating the bubble-particle collection efficiency is possible. The results showed that the bubble-particle collection efficiency increased with increasing of the S_b. Difficulty in the floating of fine particles is attributed to the low efficiency of bubble-particle collision efficiency while difficulty in the floating of coarse particles is due to high efficiency of bubble-particle detachment. According to Fig. 6, the bubble-particle collection efficiency of both the fine and coarse particles was low. So the highest bubble-particle collection efficiency was obtained for the medium size classes of -53+37, -75+53 and -106+75 μm.

CONCLOSIONS

In this research, the effect of S_b and particle size on the k of pyrite particles was investigated and the following conclusions were made:

The flotation recovery of the pyrite particles increased with increase in the S_b. Also the k increased with increase in of the S_b and decrease in of the particle size. The collision, attachment and detachment efficiencies were calculated for the different S_b and particle sizes. The maximum Stokes' collision efficiency was obtained as 81.57% with the S_b of 27.43 1/s, particle size of -500+420 μm and k of 0.22 1/min. The maximum Stokes' attachment efficiency was obtained as 50.60% with the particle size of -37 μm, S_b of 27.43 1/s and k of 0.44 1/min. The maximum detachment efficiency was obtained as 51.89% with the S_b of 16.77 1/s, particle size of -212+106 μm and k of 0.37 1/min. The bubble-particle collection efficiency increased with increasing of the S_b. So difficulty in the floating of fine particles is attributed to low efficiency of the bubble-particle collision efficiency while difficulty in the floating of coarse particles is due to high efficiency of the bubble-particle detachment.

Nomenclature

Bo^*	Bond number
C_1	Empirical value
D_{32}	Sauter mean diameter
d_b	Bubble diameter
d_p	Particle diameter
E_a	Attachment efficiency
E_{col}	Collection efficiency
E_c	Collision efficiency
E_d	Detachment efficiency
g	Acceleration due to gravity
J_g	Superficial gas velocity
k	Flotation rate constant
R	Recovery
R^*	Infinite recovery

Re_b	Bubble Reynolds number
R_f	Froth recovery factor
S_b	Bubble surface area flux
t	Time
t_i	Induction time
v_b	Bubble velocity
v_p	Particle velocity
Z	Collision frequency
Z'	Detachment frequency
α	Flotability factor
ε	Energy dissipation
η	Dynamic viscosity
ν	Kinematic viscosity
θ	Contact angle
ρ	Fluid density
ρ_s	Particle density
σ	Surface tension

Acknowledgment

Authors are grateful to Tarbiat Modares University, Amirkabir University of Technology and University of Tehran for their contribution on this research.

Received : Dec. 16, 2011 ; Accepted : Oct. 30, 2012

REFERENCES

[1] Nguyen A.V., Evans G.M., Attachment Interaction between Air Bubbles and Particles in Froth Flotation, *Experimental Thermal and Fluid Science*, **28**, p. 381 (2004).

[2] Trahar W.J., The Selective Flotation of Galena from Sphalerite with Special Reference to the Effects of Particle Size, *Int. J. Miner. Process*, **3**, p. 151 (1976).

[3] Shahbazi B., Rezai B., The Effect of Type and Dosage of Frothers on Coarse Particles Flotation, *Iranian Journal of Chemistry and Chemical Engineering*, **28**(1), p. 95 (2009).

[4] Anthony R.M., Kelsall D.F., Trahar W.J., The Effect of Particle Size on the Activation and Flotation of Sphalerite, *Proceedings of the Australian Institute of Mining and Metallurgy*, **254**, p. 47 (1975).

[5] Trahar W.J., A Rational Interpretation of the Role of Particle Size in Flotation, *Int. J. Miner. Process*, **8**, p. 289 (1981).

[6] Shahbazi B., Rezai B., Koleini S.M.J., Effect of Dimensionless Hydrodynamic Parameters on Coarse Particles Flotation, *Asian. J. Chem*, **3**, p. 2180 (2008).

[7] Shahbazi B., Rezai B., Koleini S.M.J., The Effect of Hydrodynamic Parameters on Probability of Bubble-Particle Collision and Attachment, *Miner. Eng*, **22**, p. 57 (2009).

[8] Shahbazi B., Rezai B., Koleini S.M.J., Bubble-Particle Collision and Attachment Probability on Fine Particles Flotation, Bubble-Particle Collision and Attachment Probability on Fne Particles Flotation, *Chem. Eng. Process*, **49**, p. 622 (2010).

[9] Chehreh Chelgani S., Shahbazi B., Rezai B., Estimation of Froth Flotation Recovery and Collision Probability Based on Operational Parameters Using an Artificial Neural Network, *Int. J. Min. Met. Mater*, **17**, p. 526 (2010).

[10] Shaban E. Ghazy, Ahmed H. Ragab, Removal of Lead Ions from Aqueous Solution by Sorptive-Flotation Using Limestone and Oleic Acid, *Iranian Journal of Chemistry and Chemical Engineering*, **26**(4), p. 83 (2007).

[11] Spedden H.R., Hannan W.S., Attachment of Mineral Particles to Air Bubbles in Flotation, *Min. Tech*, **12**, p. 2354 (1984).

[12] Whelan P.F., Brown D.S., Particle-Bubble Attachment in Froth Flotation, *Transactions of the Institute of Mining and Metallurgy*, **65**, p. 181 (1956).

[13] Pérez-Garibay R., Martínez-Ramos E., Rubio J., Gas Dispersion Measurements in Microbubble Flotation Systems, *Miner Eng*, in press (2011).

[14] Gorain B.K., Franzidis J.P., Manlapig E.V., Studies on Impeller Type, Impeller Speed and Air Flow Rate in an Industrial Scale Flotation Cell. Part 2: Effect on Gas Holdup, *Miner. Eng*, **8**, p. 1557 (1995b).

[15] Gorain B.K., Franzidis J.P., Manlapig E.V., Studies on Impeller Type, Impeller Speed and Air Flow Rate in an Industrial Scale Flotation Cell. Part 3: Effect on Superficial Gas Velocity, *Miner. Eng*, **9**, p. 639 (1996).

[16] Gorain B.K., Franzidis J.P., Manlapig E.V., The Effect of Gas Dispersion Properties on the Kinetics of Flotation. Column 96, "35th Annual Conference of Metallurgists", CIM, Montreal, Canada, 299-313 (1996b).

[17] Gorain B.K., Franzidis J.P., Manlapig E.V., Studies on Impeller Type, Impeller Speed and Air Flow Rate in an Industrial Scale Flotation Cell. Part 4: Effect of Bubble Surface Area Flux on Flotation Kinetics, *Miner. Eng*, **10**, p. 367 (1997).

[18] Gorain B.K., Franzidis J.P., Manlapig E.V., Studies on Impeller Type, Impeller Speed and Air Flow Rate in an Industrial Scale Flotation Cell. Part 5: Validation of k-Sb Relationship and Effect of Froth Depth, *Miner. Eng*, **11**, p. 615 (1998).

[19] Hernandez-Aguilar J.R., Rao S.R., Finch J.A., Testing the k-Sb Relationship at the Microscale, *Miner. Eng*, **18**, p. 591 (2005).

[20] Girgin E.H., Do S., Gomez C.O., Finch J.A., Bubble Size as a Function of Impeller Speed in a Self-Aeration Laboratory Flotation Cell, *Miner. Eng*, **19**, p. 201 (2006).

[21] Jameson G.J., Nam S., Young M.M., Physical Factors Affecting Recovery Rates in Flotation, *Min. Sci. Eng*, **9**, p. 103 (1977).

[22] Schulze H.J., Hydrodynamics of Bubble-Mineral Particle Collisions, *Min. Process. Extractive. Metall*, **5**, p. 43 (1989).

[23] Flint L.R., Howarth W.J., The Collision Efficiency of Small Particles with Spherical Air Bubbles, *Chem. Eng. Sci*, **26**, p. 1155 (1971).

[24] Yoon R.H., The Role of Hydrodynamic and Surface Forces in Bubble-Particle Interaction, *Int. J. Miner. Process*, **58**, p. 129 (2000).

[25] Saffman P.G., Turner T.S., On the Collision of Drops in Turbulent Clouds, *J Fluid Mech*, **1**, p. 16 (1956).

[26] Nguyen, A.V., Ralston, J., Schulze, H.J., On Modeling of Bubble-Particle Attachment Probability in Flotation, *Miner Eng*, **53**, p. 225 (1998).

[27] Bloom F., Heindel T.J., Modeling Flotation Separation in a Semibatch Process, *Chem Eng Sci*, **58**, p. 353 (2003).

[28] Mika T.S., Fuerstenau D.W., A Microscopic Model of the Flotation Process, "Eighth Int J Miner Process Congress", Leningrad, p. 246 (1968).

[29] Rodrigues R.T., Rubio J., New Basis for Measuring the Size Distribution of Bubbles, *Miner Eng*., **16**, p. 757 (2003).

[30] Dukhin S.S., Miller R., Loglio G., Physico-Chemical Hydrodynamics of Rising Bubble, Drops and Bubbles in: "Interfacial Research", Mobius D., Miller R. (Editors), Elsevier Science B.V. (1998).

[31] Schulze H.J., Physico-Chemical Elementary Processes in Flotation-An Analysis from the Point of View of Colloid Science Including Processes Engineering Considerations, *Int. J. Miner. Process,* **4**, p. 348 (1984).

[32] Bruce H.K., "Modeling of Hindered-Settling Column Separations", *A PhD Thesis in Mineral Processing*, The Pennsylvania State University, 11-13 (2003).

[33] Hu Y., Qiu G., Miller J.D., Hydrodynamic Interactions between Particles in Aggregation and Flotation, *Int. J. Miner. Process*, **70**, p. 157 (2003).

[34] Koh P.T.L., Schwarze M.P., CFD Modelling of Bubble-Particle Attachments in Flotation Cells, *Miner Eng*, **19**, p. 619 (2006).

[35] Dai Z., Fornasiero D., Ralston J., Particle-Bubble Attachment in Mineral Flotation, *Journal of Colloid and Interface Science*, **217**, p. 70 (1999).